Frequency Control using Cooperative Demand Response through Accumulated Energy

Miloš Cvetković, *Member, IEEE,* and Anuradha M. Annaswamy, *Fellow, IEEE*

***Abstract*—This paper proposes a hierarchical control architecture for engaging demand into providing primary frequency response services. The proposed architecture relies on the use of information about accumulated energy for the aggregation of demand capabilities and dissagregation of demand responsibilities. Since the accumulated energy has a distinct additive property, the aggregation/disaggregation of demand becomes straightforward. Additional unique features of the proposed architecture are that it: i) includes the information of inflexible load in the aggregated demand, ii) allows for intuitive cooperation between load aggregators. Conditions for stability under cooperating load aggregators are derived. Finally, simulations are carried out on the IEEE 39-bus system to illustrate the proposed concepts of aggregation, disaggregation and cooperation.**

***Index Terms*—Demand aggregation, primary frequency response, accumulated energy.**

I. Introduction

DEMAND response has been widely regarded as one of the key enablers for accommodating high power production by renewable resources [1]. The potential for adjusting consumption to match the volatile power production exists on all time scales. Of particular interest to this paper is demand response for providing primary frequency response.

To enable demand response on the fast time scales, novel approaches for control of flexible demand are being proposed in the literature. The research in this field has mainly evolved in two directions: i) methods intended for system operators (SOs) to include demand response units in their real-time operations [2]-[4], ii) methods intended for load serving entities (LSEs) to adequately control large number of individual flexible units [5]-[6]. References [2], [3] set up the frequency correction problem as an optimization problem with either economic [2] or technical [3] objectives. In [4], a discrete-time form of an economically optimal demand controller is proposed. Controlling large number of demand responsive units using mean field games has been explored for the case of pool pumps in [5]. An approach using Markov chain model for control of thermostatically controlled loads (TLCs) has been reported in [6]. Decentralized response to real-time frequency deviation is a common characteristic of all these methods. Due to the decentralized nature of the control algorithms, SO- and LSE-level decision making has to be carefully integrated to avoid undesired destabilizing effects on the system frequency.

Control architectures that combine both SO- and LSE-level decision making have been less commonly reported. In [7] and [8] the authors describe a hierarchical control architecture that consists of centralized droop design at the SO-level and of distributed scheduling of individual demand switching at the LSE-level. This paper proposes an alternative hierarchical control architecture that combines the participation of both SO- and LSE-entities in providing primary frequency control using responsive demand.

One of the key challenges for designing efficient demand response control architecture is aggregation and disaggregation of demand into coherent controllable units. The aggregation is often performed using stochastic methods and by assuming large number of adjustable loads [5], [6]. The aggregated models, thus, could show limited performance when the number of participating responsive loads is relatively small. This scenario is of particular importance during early adoption stages with low demand participation. The architecture proposed in this paper is focused on enabling simple aggregation of demand capabilities and disaggregation of demand responsibilities across heterogeneous demand units.

As demand response programs become more widespread, sharing responsibilities between different LSEs becomes crucial for guaranteeing adequate frequency response. This paper proposes an accumulated energy-based approach to modeling of demand responsive units that lends itself to an algorithm for cooperation between LSEs, and the overall hierarchical control architecture.

A. Proposed Approach

Accumulated energy is a strong indicator of stability of interconnected power systems [9]. Hamiltonian-based approaches have been applied to assess power system stability in the past [10]. More recently, control of power system components using energy has been investigated in [11]. In this reference, power system components are represented using accumulated energy as one of the component states. The same approach has been applied in this paper to model electricity demand using energy state variables.

Besides being intuitive for stability assessment, the main attribute of accumulated energy that is heavily exploited in this paper is its additivity. Additivity refers to the property of energy by which accumulated energy E_j of component j is equal to the sum of accumulated energies $E_j^{(k)}$ of all of its subcomponents $k = 1, \dots N$, i.e.

$$E_j = \sum_{k=1}^{N} E_j^{(k)} \tag{1}$$

Department of Mechanical Engineering, Massachusetts Institute of Technology, Cambridge, MA, {mcvetkov,aanna}@mit.edu

This work was supported by the NSF initiative, Award no. EFRI-1441301.

Equation (1) allows for straightforward combination of accumulated energy states, while downplaying the topology connections between different loads. This feature is extremely useful for aggregation and disaggregation of demand capabilities under one LSE. Additionally, this property provides foundation for cooperation between different LSEs and enables them to combine their efforts in the situations when they cannot fulfill their responsibilities individually. To obtain better load model accuracy, the information on the inflexible load is included in the aggregated demand model in this paper.

The rest of the paper is organized as follows. Section II describes an integrated inflexible and flexible load model, establishes its representation using energy states, and finally, presents the system model in the energy-power state space. Section III explains aggregation and disaggregation using energy framework. In Section IV, a method for cooperation between LSEs is presented. Finally, Section V shows results of numerical simulations.

II. Modeling

Starting from the typical load representation for power system stability studies, this section introduces an integrated inflexible and flexible load model in a form suitable for later use. Next, this model is converted to the accumulated energy state space representation. Finally, the complete power system model in accumulated energy state space is derived.

A. Integrated Inflexible and Flexible Demand Model

According to [12], at any given time any inflexible load at some node in the grid can be represented as a composition of constant impedance load, constant current load and constant power load as in (2).

$$P_{IL_\omega} = P_{IL_0}\left[p_{il_1}\frac{V^2}{V_0^2} + p_{il_2}\frac{V}{V_0} + p_{il_3}\right](1 + K_{IL}\Delta\omega) \quad (2)$$

In this model, p_{il_1}, p_{il_2} and p_{il_3} are the ratios of constant impedance, current and power, which satisfy $p_{il_1}+p_{il_2}+p_{il_3} = 1$, while P_{IL_0} represents the nominal value of the composite load at the particular time of interest. Load voltage level is given by V while its nominal value is given by V_0. Finally, the sensitivity of the load to the change in frequency $\Delta\omega$ is given by the coefficient K_{IL}. Note that machine loads are not covered by the representation (2) and will be introduced in what follows.

Model (2) is a standard load model used in power system dynamic studies [13] and its parameters can be estimated in real-time [14] at the order of hundreds of milliseconds. Since the focus of this paper is on the frequency control, the load model from (2) is represented as

$$P_{IL_\omega} = P_{IL}(1 + K_{IL}\Delta\omega) \quad (3)$$

where $P_{IL} = const$ by assuming constant voltage level throughout the grid. Reference [6] shows that constant voltage assumption results in an error not higher than 2% for the method proposed therein. This paper recognizes the existence of such error but does not investigate its impact due to limited space.

Flexible demand is often portrayed in the same form [8]

$$P_{FD_\omega} = P_{FD}(1 + K_{FD}\Delta\omega) \quad (4)$$

where P_{FD} is the active power consumed by the flexible demand and K_{FD} is the sensitivity of the flexible demand to the frequency deviation. Both of these values are adjustable by the corresponding LSE. The composition of the participating flexible units could be diverse, and their actual switching logic may vary correspondingly. Physical characteristics of consumption [15] will determine accuracy of achieving K_{FD} with many adjustable loads. Under the assumption that the number of participating flexible units is large and that they can be exactly controlled at any given time, K_{FD} could take any value from $K_{FD} \in \mathcal{D}_\mathcal{K}$. Such assumption is made in this paper.

The integrated load model is created by combining (3) and (4) into

$$P_{IL_\omega} + P_{FD_\omega} = P_L + P_L\left(p_{il}K_{IL} + p_{fd}K_{FD}\right)\Delta\omega \quad (5)$$

where $P_L = P_{IL} + P_{FD}$, $p_{il} = \frac{P_{IL}}{P_L}$ and $p_{fd} = \frac{P_{FD}}{P_L}$, while $p_{il} + p_{fd} = 1$.

B. Accumulated Energy Model of the Load

The load model given in (5) is a steady state model that does not capture the rate of response of the load to the change in frequency. The notion of synthetic inertia, denoted by $J_{L_{syn}} \in \mathbb{R}^+$, is introduced in this paper to assign the information on the response rate to the load model. As the name suggests, this inertia does not represent the physical inertia of controllable devices. Instead, it originates from the inherit delays of the control method used and the granularity of power steps that can be achieved with the participating flexible demand units. In this paper, it is assumed that $J_{L_{syn}}$ is constant over the period of interest.

A group of loads unmentioned so far are machine loads which are modeled with their physical inertia constant $J_{L_{phy}}$. These devices, controllable or uncontrollable, can be aggregated with the loads represented using composite load model by adding the two inertia constants together to obtain $J_L = J_{L_{syn}} + J_{L_{phy}}$.

Finally, the accumulated energy of the load j is defined as

$$E_{L_j} := \frac{1}{2}J_{L_j}\omega^2 \quad (6)$$

which yields $\Delta E_{L_j} = J_{L_j}\omega_0\Delta\omega$ when linearized around ω_0. From here on, small deviation notation Δ is dropped in all expressions for simplicity. Additionally, it is assumed that all variables are given in per units, which yields $\omega_0 = 1$.

By noting that the first derivative of energy has the dimension of power, i.e. $\dot{E} = P$, it follows from (5) and (6) that the load model in the energy domain can be described as

$$\dot{E}_{L_j} = \sum_{k\in\mathcal{F}_n} P_{f_{kj}} - P_{L_j} - \frac{D_{L_j}}{J_{L_j}}E_{L_j} \quad (7)$$

where $D_{L_j} = P_{L_j}(p_{il_j}K_{IL_j} + p_{fd_j}K_{FD_j})$ and $\mathcal{F}_n$ is the set of all line flows meeting at node j and accounted for as

positive if their assigned direction is into the node and negative otherwise.

Dynamic model (7) represents the load model in accumulated energy domain parametrized by the synthetic inertia constant J_{L_j}, and the synthetic damping coefficient D_{L_j}. Parameters $J_{L_j} \in \mathcal{D}_{\mathcal{J}}$ and $D_{L_j} \in \mathcal{D}_{\mathcal{D}}$ are adjusted by the corresponding LSE. Also note that the assumption of frequency sensitive nodes from [2], [16] is replaced by the property of loads to accumulate energy.

C. Power System Model in Energy Domain

First, the generator model is introduced. The classical generator model captures dynamics of mechanical frequency rotation of generator i as

$$\dot{\omega}_i = \frac{1}{J_{G_i}}(P_{M_i} - \sum_{k \in \mathcal{F}_n} P_{f_{ik}} - D_{G_i}\omega_i) \tag{8}$$

where J_{G_i} is the inertia of generator i, D_i its damping coefficient, P_{M_i} its mechanical power input.

The energy model of a generator can be established in a similar fashion as the one of the load, i.e. by substituting state ω_i with the accumulated energy of the generator E_{G_i}.

$$\dot{E}_{G_i} = P_{M_i} - \sum_{k \in \mathcal{F}_n} P_{f_{ik}} - \frac{D_{G_i}}{J_{G_i}} E_{G_i} \tag{9}$$

A linearized active power model that appeared in [17], [3] is used to represent the transmission system. This model assumes constant voltage levels across the grid, small voltage phase angle differences and negligible losses. Transmission lines are represented using linearized flow variable dynamics

$$\dot{P}_{f_{nm}} = B_{nm}(\omega_n - \omega_m) \tag{10}$$

where B_{nm} is the susceptance of the transmission line between nodes n and m.

Transmission line flows can be expressed in terms of accumulated energy at the nodes as

$$\dot{P}_{f_{nm}} = B_{nm}(\frac{E_n}{J_n} - \frac{E_m}{J_m}) \tag{11}$$

Finally, the power grid is modeled as an undirected graph whose nodes belong either to $\mathcal{G}$ or $\mathcal{L}$. Those nodes without generation or demand can be reduced from the grid using Kron's reduction [18]. Transmission lines belong to the set $\mathcal{T}$. Thus, a power grid model can be stated as

$$\begin{aligned}
\dot{E}_{G_i} &= P_{M_i} - \sum_{k \in \mathcal{F}_i} P_{f_{ik}} - \frac{D_{G_i}}{J_{G_i}} E_{G_i} \quad i \in \mathcal{G} \\
\dot{E}_{L_j} &= \sum_{k \in \mathcal{F}_j} P_{f_{kj}} - P_{L_j} - \frac{D_{L_j}}{J_{L_j}} E_{L_j} \quad j \in \mathcal{L} \\
\dot{P}_{f_{nm}} &= B_{nm}(\frac{E_n}{J_n} - \frac{E_m}{J_m}) \quad (n,m) \in \mathcal{T}
\end{aligned} \tag{12}$$

III. Aggregation and Disaggregation within LSE

The aggregation and disaggregation are based on the control architecture in Figure 1 that is to some extent implicitly assumed in [3], [5], [6] while explicitly stated in [7], [8]. In this architecture, the LSE collects the information about load capabilities from the individual units and combines it together. This process is referred to as *aggregation*. The aggregated information on load capabilities, denoted by J_{L_j} and $\mathcal{D}_{D_j}$, is communicated from the LSEs to the SO at a rate from tens of minutes to an hour. The SO uses this information to compute the actual damping coefficient D_j for each of the nodes. This computation can be performed using heuristics from [8] or any other adequate analytical method. The newly obtained D_{L_j} coefficients are communicated to the LSEs. Assigning the responsibilities to individual loads based on the assigned D_{L_j} is referred to as *disaggregation*. Since it is assumed that the SO already knows fixed D_{G_i}/J_{G_i} of all generators, this type of architecture ensures that droop constants K_{FD_j} of flexible demand are aligned with droop constants of generator prime movers.

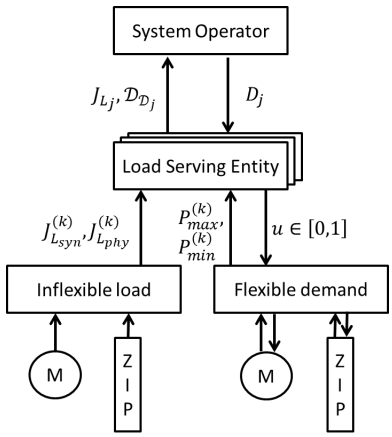

Fig. 1. A hierarchical control architecture for demand response.

Aggregation: Let load at bus j be composed of N integrated loads that are modeled as in (5), and let $J^{(k)}_{L_j}$ where $k = 1 \dots N$ denote the synthetic inertia constants of the N loads. The synthetic inertia of the aggregated load is computed as the sum

$$J_{L_j} = \sum_{k=1}^{N} J^{(k)}_{L_j} \tag{13}$$

Relationship (13) follows directly from energy definition (6) and the additivity property of energy (1).

Disaggregation: Let load at bus j be composed of N integrated loads that are modeled as in (5), and let $K^{(k)}_{FD_j}$ where $k = 1..N$ denote the droop constants of the N loads and $P^{(k)}_{FD_j}$ be their active power operating levels. The droop constants of the integrated loads have to satisfy the following relationship

$$D_{L_j} - P_{IL_j} K_{IL_j} = \sum_{k=1}^{N} P^{(k)}_{FD_j} K^{(k)}_{FD_j} \tag{14}$$

Relationship (14) follows directly from energy definition (6) and the additivity property of energy (1).

The actual values for $K_{FD_j}^{(k)}$ are computed by the corresponding LSE during disaggregation to optimize either technical or economic performance of flexible demand. For example, higher value for $K_{FD_j}^{(k)}$ can be assigned to the integrated load that possesses higher number of participating units which would result in better realization of the assigned damping coefficient.

Note that an LSE could internally reevaluate $K_{FD_j}^{(k)}$ coefficients with a period higher than the operating interval T. This ensures a level of flexibility to the changing operating conditions. If such reevaluation does not provide expected benefits, reevaluation through cooperation with another LSE can be used instead, which is addressed in Section IV.

IV. Cooperation between LSEs

Since the aggregation of demand capabilities and disaggregation of demand responsibilities are performed at a rate of tens of minutes to hours, which is denoted here by T, an emergency mechanism is needed to share the assignments between LSEs in the case operating conditions change considerably within T. Cooperation between LSEs that exchange accumulated energy information is a mechanism that ensures satisfying demand behavior in response to frequency deviation.

In what follows, it is assumed that two cooperating LSEs, A and B, are also neighboring LSEs, i.e. there exist at least one transmission line whose one terminal node j belongs to LSE A and the other terminal node k belongs to LSE B.

Cooperation: Let two neighboring LSEs, A and B, be assigned with K_{FD_j} and K_{FD_k} for their respective nodes at the beginning of an operating interval T. Assume that LSE A is capable of delivering only $K'_{FD_j} < K_{FD_j}$ due to a sudden lack of demand responsive units in its jurisdiction. If LSE B reevaluates its droop coefficient K'_{FD_k} by solving for new D'_{L_k} using the following relationship

$$\frac{D'_{L_j}}{J'_{L_j}} + \frac{D'_{L_k}}{J_{L_k}} + \frac{\sqrt{D'_{L_j} D'_{L_k}}}{\sqrt{J'_{L_j} J_{L_k}}} = D_{L_e} \tag{15}$$

where D_{L_e} is computed as $D_{L_e} = \frac{D_{L_j}}{J_{L_j}} + \frac{D_{L_k}}{J_{L_k}} + \frac{\sqrt{D_{L_j} D_{L_k}}}{\sqrt{J_{L_j} J_{L_k}}}$ then the sufficiently high damping K'_{FD_k} of the LSE B that can compensate for the lack of performance of the LSE A is guaranteed.

Proof: Since LSE A cannot perform according to the assigned responsibility K_{FD_j}, the energies of the loads j and k of the two LSEs are combined into a single state $E_{L_e} = E_{L_j} + E_{L_k}$. Dynamic behavior of this state is described by

$$\dot{E}_{L_e} = \sum_{i \in \mathcal{F}_j \cup \mathcal{F}_k} P_{f_{ie}} - (P_{L_j} + P_{L_k}) - \frac{D_{L_e}}{J_{L_j}} E_{L_e} \tag{16}$$

where D_{L_e} is computed as in (15) so that the last term of (16) satisfies

$$\begin{aligned} &|| \frac{D'_{L_j}}{J'_{L_j}} E_{L_j} + \frac{D'_{L_k}}{J_{L_k}} E_{L_k} || \leq \\ &|| \left(\frac{D'_{L_j}}{J'_{L_j}} + \frac{D'_{L_k}}{J_{L_k}} + 2 \frac{\sqrt{D'_{L_j} D'_{L_k} E_{L_j} E_{L_k}}}{E_{L_e} \sqrt{J'_{L_j} J_{L_k}}} \right) E_{L_e} || \leq \\ &|| \left(\frac{D'_{L_j}}{J'_{L_j}} + \frac{D'_{L_k}}{J_{L_k}} + \frac{\sqrt{D'_{L_j} D'_{L_k}}}{\sqrt{J'_{L_j} J_{L_k}}} \right) E_{L_e} || \end{aligned} \tag{17}$$

A. Stability Conditions for Cooperation

Stability conditions for cooperation are based on the connective stability concepts from [19]. Power system model (12) can be represented in a connective form as

$$\begin{aligned} \dot{x}_1 &= A_{11} x_1 + A_{12} x_2 \\ \dot{x}_2 &= A_{22} x_2 + A_{21} x_1 \end{aligned} \tag{18}$$

where $x_2 = E_{L_e}$ is the aggregated energy of LSE A and B, and vector x_1 contains all other states of the system.

Theorem: System (18) is stable if the systems $\dot{x}_1 = A_{11} x_1$, $\dot{x}_2 = A_{22} x_2$, and $\dot{r} = W r$ are stable, where W is defined as

$$w_{ij} = \begin{cases} -\frac{\lambda_m(G_i)}{2\lambda_M(H_i)} & , \quad i = j \\ \frac{\sqrt{\lambda_M(A_{ij}^T A_{ij})}\lambda_M(H_i)}{\sqrt{\lambda_m(H_j)}\sqrt{\lambda_m(H_i)}} & , \quad i \neq j \end{cases} \quad i,j = 1,2 \tag{19}$$

and where $\lambda_m(\cdot)$ and $\lambda_M(\cdot)$ are the minimum and maximum eigenvalue, and H_k and G_k are positive semidefinite matrices that satisfy $A_{11}^T H_1 + H_1 A_{11} = -G_1$ and $A_{22}^T H_2 + H_2 A_{22} = -G_2$.

Proof: See [19] for proof.

Theorem: System (18) is stable iff its two subsystems A_{11} and A_{22} are stable and if the following relationship holds

$$\frac{\lambda_m(G_1)\lambda_m(H_1)}{\lambda_M^2(H_1)} > \frac{4\lambda_M^2(H_2)\sqrt{\lambda_M(A_{12}^T A_{12})\lambda_M(A_{21}^T A_{21})}}{\lambda_m(G_2)\lambda_m(H_2)} \tag{20}$$

Proof: Condition (20) can be rewritten as $w_{11} w_{22} - w_{12} w_{21} > 0$. Since $w_{ij} \leq 0$ for $i = j$ and $w_{ij} \geq 0$ for $i \neq j$, condition (20) is necessary and sufficient to have negative poles of matrix W, and thus, stability of system (18).

Theorem: System (18) is stable iff D_{L_e} satisfies the following relationship

$$D_{L_e} < \frac{J_{L_e} K}{8\sqrt{\lambda_M(A_{12}^T A_{12})\lambda_M(A_{21}^T A_{21})}} \tag{21}$$

where $K = \frac{\lambda_m(G_1)\lambda_m(H_1)}{\lambda_M^2(H_1)}$.

Proof: Relationship (21) follows from (20) by setting $\frac{\lambda_M(H_2)}{\lambda_m(H_2)} = 1$ and $\frac{\lambda_M(H_2)}{\lambda_m(G_2)} = 2\frac{D_{L_e}}{J_{L_e}}$.

Relationship (21) can be extremely useful in practice to ensure that the damping coefficient obtained through cooperation between two LSEs does not violate stability conditions of the whole system. To successfully perform this check, SO needs to supply constant K to the cooperating LSEs.

V. Simulation Results

Simulations are performed on the IEEE 39-bus system to illustrate aggregation, disaggregation and cooperation. This system has 10 generator and 19 load nodes. The remaining nodes are reduced using Kron's reduction. Parameters of the IEEE 39-bus transmission grid B_{nm} and the dynamic parameters of the generators D_{G_i} and J_{G_i} are taken from [20]. Nominal mechanical power input of generators P_{M_i} and nominal load consumption P_{L_j} are also taken from this reference. Frequency damping coefficient of inflexible loads K_{IL_j} have been assigned to loads randomly in the range $[0, 1]$ as suggested in [12].

The nominal level of flexible demand on all consumption nodes P_{FD_j} is taken in a random fashion as a percentage of total nominal load P_{L_j} ranging between $20\% - 30\%$, i.e. $p_{fd_j} \in [0.2, 0.3]$. The nominal level of inflexible load on all consumption nodes P_{IL_j} is computed as $P_{IL_j} = p_{il_j} P_{L_j}$ where $p_{il_j} = 1 - p_{fd_j}$. Synthetic inertia constants J_{L_j} are randomly chosen in the range $[0, 0.3]$ which is at least two order of magnitudes less than the smallest J_{G_i}.

To illustrate aggregation, disaggregation and cooperation the attention is focused on two nodes, namely 15 and 16. Load at bus 15 is composed of an inflexible load component, and two controllable components which are thermostatically controlled loads (TCLs) and pool pumps as shown in Figure 2. In the same figure, load at bus 16 is composed of inflexible load component and thermostatically controlled loads. It is further assumed that bus 15 belongs to LSE A and that bus 16 belongs to LSE B.

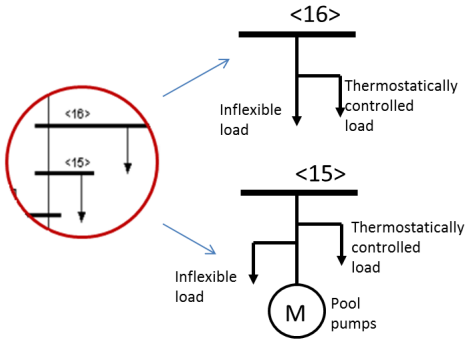

Fig. 2. Composition of load on nodes 15 and 16 in the IEEE 39-bus system.

In these simulations, disturbance is simulated as a random deviation in nominal power of inflexible load, i.e. $P_{L_j} + \mathcal{U}(-0.5, 0.5)$MW. Figure 3(a) shows the impact of this disturbance on the system frequency if $K_{FD_j} = 0, \forall j \in \mathcal{L}$. This simulation is performed to illustrate the base case, when no flexible demand exists in the grid.

At the beginning of an operating interval, the SO will collect the load capability parameters from the LSEs and will compute new damping coefficients D_{L_j} which yield K_{FD_j}. Relevant parameters of the loads on these particular nodes for the operating period of interest are given in Table I.

Figure 3(b) shows the response of the system frequency to the same disturbance with assigned droop coefficients of

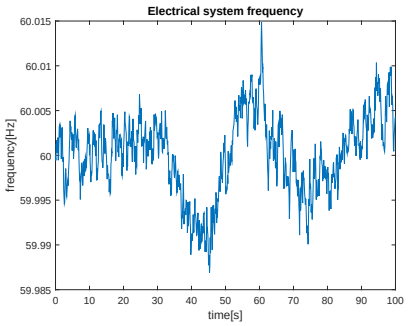

(a) Without flexible demand

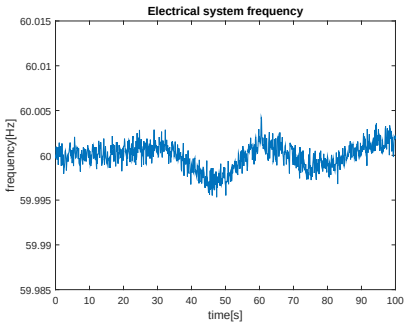

(b) With flexible demand

Fig. 3. Electrical frequency response in the IEEE 39-bus system.

TABLE I
Parameters of the load on nodes 15 and 16.

Node	15	16
J_{L_j}	0.1153	0.0288
D_{L_j}	2.3672	3.1146
K_{IL_j}	0.7140	0.9604
K_{FD_j}	0.7485	0.9426
p_{il_j}	0.2545	0.2286
p_{fd_j}	0.7455	0.7714

flexible demand K_{FD_j} for $j = 15, 16$ as in Table I. The frequency deviation is much smaller when flexible demand is engaged in its stabilization.

To illustrate disaggregation, it is assumed that the number of pool pumps at node 15 has decreased by one half during the operating hour. This results in 50% change of the inertia of the aggregated demand at node 15 and in 25% decrease of $K_{FD_{15}}$. The accumulated energy response is given in Figure 4(a).

As explained previously, the LSE will internally reevaluate its droop characteristic $K_{FD_{15}}$ by readjusting the droop of the TCLs. Figure 4(b) shows the same accumulated energy signal after reevaluation of $K_{FD_{15}}$. High frequency fluctuations of accumulated energy are smoothed out with the reevaluated parameters.

Next, a case is considered in which LSE A cannot reevaluate the droop coefficient for load at node 15 and instead engages in cooperation with LSE B. In this case, LSE B will reevaluate its droop coefficient as described earlier obtaining $D_{L_{16}} = 5.2955$ $K_{FD_{16}} = 1.8020$. Figure 5(a) shows the response of the accumulated energy of the load at node 16 without the adjustment while Figure 5(b) shows the response of the same variable with the reevaluated coefficients. After reevaluation,

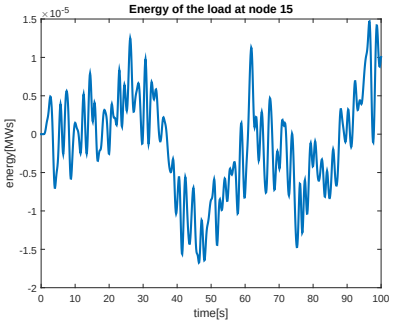

(a) Without reevaluation of droop characteristic

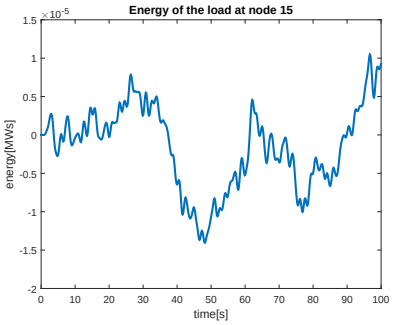

(b) With reevaluation of droop characteristic

Fig. 4. Accumulated energy of the load at node 15 in response to decreased performance by pool pumps.

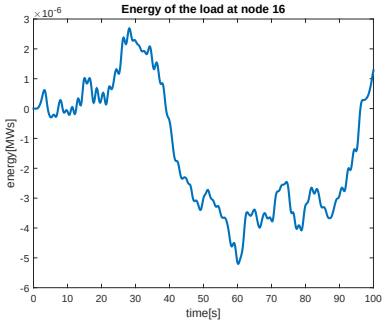

(a) Without cooperation between LSEs

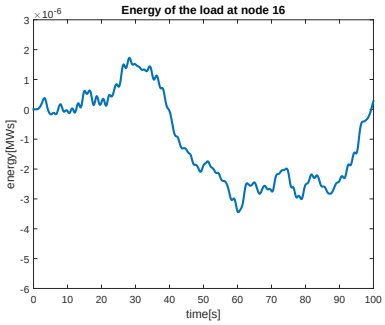

(b) With cooperation between LSEs

Fig. 5. Accumulated energy of the load at node 16 in response to decreased performance by pool pumps.

LSE 16 is engaging more resources which results in lower accumulated energy deviation.

Finally, the average benefit obtained through cooperation is quantified by comparing the degradation of frequency stabilization performance due to the reduction in flexible demand at node 15 with the improvement obtained through cooperation with flexible demand at node 16. Degradation and improvement are compared for 10 different values of flexible demand reduction $K'_{FD_{15}}$ ranging from 0% to 100% of $K_{FD_{15}}$ from Table I in 10% increments. Both, degradation and improvement are quantified using disparity ratio which is computed as $\frac{\mathbb{E}(x-x')^2}{\mathbb{E}(x^2)} + \frac{\mathbb{E}(y-y')^2}{\mathbb{E}(y^2)}$, where $x = E_{L_{15}}$ and $y = E_{L_{16}}$ for the case with load reduction but without cooperation. When computing degradation $x' = E_{L_{15}}$ and $y' = E_{L_{16}}$ take values for the case without load reduction. When computing improvement $x' = E_{L_{15}}$ and $y' = E_{L_{16}}$ take values for the case with demand cooperation.

Figure 6 shows the obtained values for degradation and improvement. Both, degradation and improvement are in the range between 9% and 23%. In all cases but one, the improvement using cooperation is higher than the degradation faced by the loss of responsive demand. The difference between the two is much more significant for a lower percentage of lost demand.

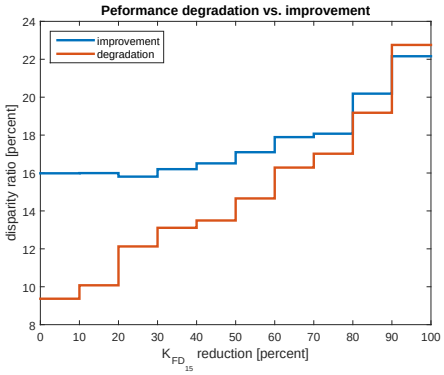

Fig. 6. Degradation due to flexible demand loss vs. improvement through cooperation.

VI. Conclusions

This paper introduces an energy-based modeling approach for aggregation and disaggregation of demand within one LSE and a method for cooperation between two LSEs. The additivity of accumulated energy is exploited to simplify these objectives. The model has been tested on the IEEE 39-bus system. It was shown that aggregation, disaggregation and cooperation lead to smoother frequency and accumulated energy response. A 16 to 23% improvement was obtained using our approach and its aggregation-disaggregation-cooperation components. Future work will further investigate imperfections in control of demand by including more accurate models of LSE-level control.

References

[1] Chuang, A.S.; Gelling, C.W.; *Demand-side Integration in a Restructured Electric Power Industry*, CIGRE General Session, Paris, France, August 24-29, 2008.

[2] Zhao, C.; Topcu, U.; Low, S.H., *Optimal Load Control via Frequency Measurement and Neighborhood Area Communication*, in Power Systems, IEEE Transactions on , vol.28, no.4, pp.3576-3587, Nov. 2013.

[3] Zhao, C.; Topcu, U.; Li, N.; Low, S.H., *Design and Stability of Load-Side Primary Frequency Control in Power Systems*, in Automatic Control, IEEE Transactions on , vol.59, no.5, pp.1177-1189, May. 2014.
[4] Shiltz, D.; Annaswamy, A.M., *A Practical Integration of Automatic Generation Control and Demand Response*, IEEE American Control Conference, Boston 2016, (submitted).
[5] Meyn, S.; Barooah, P.; Busic, A.; Chen, Y.; Ehren, J., *Ancillary Service to the Grid Using Intelligent Deferrable Loads*, in Automatic Control, IEEE Transactions on , doi: 10.1109/TAC.2015.2414772.
[6] Mathieu, J.L.; Koch, S.; Callaway, D.S., *State Estimation and Control of Electric Loads to Manage Real-Time Energy Imbalance*, in Power Systems, IEEE Transactions on , vol.28, no.1, pp.430-440, Feb. 2013.
[7] Kalsi, K.; Elizondo, M.; Lian, J.; Zhang, W.; Marinovici, L.D.; Moya, C., *Loads as a Resource: Frequency Responsive Demand*, PNNL-SA-23764, September 2014.
[8] Elizondo, M.A.; Kalsi, K.; Calderon, C.M.; Zhang, W., *Frequency Responsive Demand in U.S. Western Power System Model*, in PES General Meeting, 2015 IEEE , 27-31 July 2015.
[9] Pai, M.A., *Energy Function Analysis for Power System Stability*, Kluwer Academic Publishers, 1989.
[10] Vittal, V.; Michel, A.N.; Fouad, A.A., *Power System Transient Stability Analysis: Formulation as Nearly Hamiltonian Systems*, in American Control Conference, 1983 , vol., no., pp.668-673, 22-24 June 1983.
[11] Cvetkovic, M.; Ilic, M.; *Cooperative Line-flow Power Electronics Control for Transient Stabilization*, in Conference on Decision and Control, 2014 IEEE, December 2014.
[12] Concordia, C.; Ihara, S., *Load Representation in Power System Stability Studies*, in Power Apparatus and Systems, IEEE Transactions on , vol.PAS-101, no.4, pp.969-977, April 1982.
[13] Shetye, K.S.; Overbye, T.J.; Doern, T.L., *Assessment of Discrepancies in Load Models across Transient Stability Software Packages*, in PES General Meeting, 2015 IEEE , 27-31 July 2015.
[14] Yu, S.; Zhang, S.; Han, Y.; Lu, C.; Yu, Z.; Zhang, X., *Fast Parameter Identification and Modeling of Electric Load Based on Simplified Composite Load Model*, in PES General Meeting, 2015 IEEE , 27-31 July 2015.
[15] Hansen, J.; Knudsen, J.; Annaswamy, A.M., *A Dynamic Market Mechanism for Integration of Renewables and Demand Response*, in Control Systems Technology, IEEE Transactions on, to appear, DOI 10.1109/TCST.2015.2476785.
[16] Bergen, A.R.; Vittal, V, *Power Systems Analysis*, 2nd ed. Englewood Cliffs, NJ, USA: Prentice-Hall, 2000.
[17] Zaborszky, J.; Ilic, M., *Dynamics and Control of Large Electric Power Systems*, John Wiley & Sons, 2000.
[18] Dorfler, F.; Bullo, F., *Kron Reduction of Graphs With Applications to Electrical Networks*, in Circuits and Systems I: Regular Papers, IEEE Transactions on , vol.60, no.1, pp.150-163, Jan. 2013.
[19] Siljak, D., *Large-scale Dynamic Systems: Stability and Structure*, Dover Publications, 1978.
[20] Athay, T.; Podmore, R.; Virmani, S., *A Practical Method for the Direct Analysis of Transient Stability*, in Power Apparatus and Systems, IEEE Transactions on, vol.PAS-98, no.2, pp.573-584, Mar./Apr. 1979.